Since January 2020 Elsevier has created a COVID-19 resource centre with free information in English and Mandarin on the novel coronavirus COVID-19. The COVID-19 resource centre is hosted on Elsevier Connect, the company's public news and information website.

Building and Environment 205 (2021) 108236

Contents lists available at ScienceDirect

Building and Environment

journal homepage: www.elsevier.com/locate/buildenv

Development of wearable air-conditioned mask for personal thermal management

Wing Sze Suen, Guanghan Huang, Zhanxiao Kang, Yuheng Gu, Jintu Fan, Dahua Shou *

Institute of Textiles and Clothing, The Hong Kong Polytechnic University, Kowloon, Hong Kong, China

ARTICLE INFO

Keywords:
Thermal management
Wearable technology
Mask
Comfort

ABSTRACT

A mask that creates a physical barrier to protect the wearer from breathing in airborne bacteria or viruses, reducing the risk of infection in polluted air and potentially contaminated environments, has become a daily necessity for the public especially as COVID-19 has exploded around the world. However, the use of masks often causes soaring temperatures and thick humid air, leading to thermal and wear discomfort and breathing difficulties for a number of people, and further increasing the elevated risk of heat illnesses including heat stroke and heat exhaustion. When wearers become highly active or work under high tension, the excess sweat generated negatively affects the functionality of masks. Here, we report on an innovative design of an air-conditioned mask (AC Mask) system, facilitating thermoregulation in the mask microclimate, ease of breathing, and wear comfort. The AC Mask system is developed by integrating a cost-effective and lightweight thermoelectric (TE) and ventilation unit in a wearable 3D printed mask device, compatible with existing disposable masks, to protect end users safely against toxic particles such as viruses. A wind-guided tunnel has been developed for quick and efficient ventilation of cooling air. Based on a human trial, reductions in the apparent microclimate temperature and the humidity by 3.5 °C and 50%, respectively, have been achieved under a low voltage. With the excellent thermal management properties, the AC Mask will find also wide application among professional end-users such as construction workers, firefighters, and medical personnel.

1. Introduction

Personal protective equipment (PPE) is widely utilized as in healthcare settings but the high protective insulation often reduces the performance of thermal management and wear comfort [1]. Respiratory PPE such as the filtering facepiece respirator and surgical mask (also known as medical mask) [2] has been developed to protect human beings against the inhalation of hazardous substances and infections, by filtering toxic particles, viruses, and bacteria shed in liquid droplets from the wearer's mouth and nose [3]. Surgical masks, which are widely applied to prevent the spread of viruses such as COVID-19 and influenza, have demonstrated a significant reduction (>90%) in virus detection in wearers [4]. The use of masks in the COVID-19 pandemic has been encouraged as a general measure in infection control by national governments and public health departments in East and South East Asia [5–7], while recognition of the importance of wearing a mask grows globally [8,9]. In the latest research, it has been found that wearing a mask in public is the most effective and inexpensive way of preventing inter-human transmission of viruses against the outbreak of COVID-19 [10].

Personal protective masks are generally composed of three layers, with a melt-blown microfiber filter between two spunbond fabric layers. The melt-blown layer acts as the major filter that stops microbes from entering or exiting the mask. The outer nonwoven layer is liquid-resistant and repellent to external liquid droplets and the inner nonwoven layer is skin-friendly and moisture absorbent [11]. Despite their acknowledged protection and insulation from toxins and viruses, masks have side effects of high temperatures and thick humid air that lead to significant discomfort and breathing difficulties for a substantial number of people. The air temperature within the mask greatly affects human thermal sensation [12], which is generally managed with reduced air temperature [13]. Surgical masks with improved filtration performance inevitably increase the airflow resistance passing through the mask, while the warm and moist air in the microclimate between face and mask causes condensation, consequently impairing respiratory heat loss and imposing an excessive heat burden [14]. The wet and saturated masks can also be sticky to the wearer's face and become less breathable. As well, when wearers such as construction workers, firefighters, or medical personnel become highly active or work under high

* Corresponding author.
E-mail address: dahua.shou@polyu.edu.hk (D. Shou).

https://doi.org/10.1016/j.buildenv.2021.108236
Received 1 June 2021; Received in revised form 2 August 2021; Accepted 4 August 2021
Available online 8 August 2021

Nomenclature

AH	Absolute Humidity g/m^3
AT	Apparent Temperature °C
D	Characterized length m
Re	Reynolds Number
RH	Relative Humidity
T	Temperature °C
T_d	Dewpoint Temperature °C
V	Flowing velocity m/s
ρ	Density kg/m^3
μ	dynamic viscosity Pa·s

tension, the excess heat and sweat generated within and outside a surgical mask facilitate the adherence of viruses [15] and can impair the working performance and time of wearers [16]. The hot and humid environment in tropical regimes such as Hong Kong can further increase the elevated risk of heat illness including heat stroke and heat exhaustion, becoming a problematic factor in the individual's health [17]. It has been reported that the major problems of wearing surgical masks include lack of thermal comfort and hindrance of occupational activities [14,18,19]. Moreover, current surgical masks often do not fit the wearer's face well, due to their loose fit design and frequent contact between the wetted mask and the wearer's mouth [20]. As such, it is increasingly important to develop novel surgical masks with improved thermal comfort and tolerability for the wear duration without compromising filtration performance [18,21].

Very few masks commercially available in the market have been developed to keep the wearer thermally comfortable and breathe easily. A valve-based mask [22] was developed by 3 M to release the wearer's hot exhaled breath through a valve, reducing the heat and moisture level inside the facepiece [23]. However, the risk of directly releasing viruses or toxic particles along with the breath from an infected wearer is significantly increased, such that the mask may fail to prevent the spread of virus infection [24]. As well, the mask cannot cool the wearer in an extremely hot and humid environment based on natural air ventilation. In another design, a mask coated with discontinuous patterns of phase change materials (PCM) has been developed to cool the microclimate in the internal space of the mask [25]. In particular, the cooling effect was enhanced by optimized placement of PCMs within the mask construction, and by proper arragement of the amount and density of the PCM in contact with temperature-sensitive areas of the wearer's face and areas that experienced the major airflow of the exhaled breath [25]. However, the duration of the cooling function of PCMs is always limited and they require cooling after each occasion of use, which is not cost-effective considering the required disposability in the case of highly infectious viruses such as COVID-19. To summarize, use of the masks described above is less suitable for wearers without comprehensive consideration of thermal and moisture management under the practical environment and personal conditions.

Various thermoregulation systems of active cooling have been developed and integrated into garments, including liquid cooling circulation [26], air ventilation [27–29] and PCM-encapsulated ventilation systems [30,31], in order to improve the cooling effect. Recently, a thermal mangement vest intergrated with a thermoelectric module (TE) and a hollow tubing network has been developed, supplying cooling and warming air based on the Peltier effect [32,33]. However, the study of thermoregulative mask systems is still in its infancy. In this paper, we propose to develop an innovative mask system for wear and thermal comfort, namely "Air-Conditioned Mask" (AC Mask). The AC Mask is a 3D printed frame integrated with a TE unit, allowing thermoregulative ventilation, providing sufficient space for easy breathing, and compatible with existing disposable surgical masks. It enables high protection against toxic particles such as a virus, for various end users such as individual citizens, outdoor workers, firefighters, soldiers, and medical personnel.

2. Material and methods

2.1. Development of AC mask

The AC Mask is integrated with a thermoregulation unit and 3D printed frame, compatible with disposable surgical masks, for controllable temperature and reduced humidity in the mask microclimate (Fig. 1). The illustration of the AC Mask from the front view and the side view is available in Fig. S1 and the photo of prototypes is in Fig. S2. With the 3D printed frame, direct contact between the disposable surgical mask and the wearer's nose and mouth face can be avoided, preventing the surgical mask from being wetted directly by sweat or splash from the wearer. Moreover, it provides sufficient space for air ventilation inside the mask, resulting in improved thermal and wear comfort and easy breathing. As the core component of the AC Mask, the 3D printed mask frame is made from inexpensive polylactic acid (PLA), with low weight but high tensile strength (2.7–16 GPa [34]) for the durable and stable mask support. As well, PLA is selected as the most widely used plastic filament material in 3D printing and can be economically produced from renewable resources. The dimensions of the frame are (95 ± 2) mm (L) * (112 ± 2) mm (W) with (28 ± 2) mm depth, corresponding to the Asian male head size based on the 3D anthropometric sizing analysis system. In particular, the nose protrusion has been found to be 15.8 ± 2.5 mm, so the 28-mm-depth chamber can provide good wear fit and comfort. To ensure contact fit and wear comfort, a soft, elastic silicon "sealing cushion" (SMOOTH-ON Ecoflex™ 00–30) is molded to the edge of the mask frame. Moreover, the silicone sealer can also block the penetration of external particles and viruses through the contact interface between the mask frame and the human face.

The thermoregulation unit on the basis of the Peltier effect (Fig. 2a) in the AC Mask includes a square TE module and different types of heat sink and fan in the cooling and hot sides. The TE module has two sides, and one side becomes cooler while the other gets hotter when a voltage is applied to transfer the heat. The thermoregulation unit is fixed at the bottom of the 3D printed frame, where the cooled air is supplied to reduce the temperature and humidity in the mask microclimate (Fig. 2b). To avoid bulky appearance, the dimensions of the thermoelectric system are constrained within (76 mm × 37 mm x 39 mm) ± 2 mm. On the cooling side, a tiny side blowing fan is connected to the heat exchanger to supply a flow of cool air, where the air is cooled within the heat exchanger and then blown through a 3D-printed wind-guided tunnel. The heat exchanger is made from an aluminum plate-fin heat sink covered with an impermeable copper sheet (Fig. S3a). An alternative design for the heat exchanger is integrated the plate-fin heat sink covered by tiny holes on the top surface for performance comparison (Fig. S3b). Both designs ensure that the air flow is fully cooled by the TE module without compromising the air flux. Meanwhile, a tiny fan is placed below the aluminum heat sink on the hot side for dissipation of heat to the environment. Besides its compatibility with disposable surgical masks, the AC Mask frame can be reused after sanitizing. A detailed dimension description of the thermoregulation unit is shown in Table S1, and the weight of the AC Mask is 190g exclusively with a detachable chargeable battery that can be placed in the pockets, as presented in Table S2.

To further improve the performance inside the mask, an L-shaped pipe was installed and connected with surgical mask and the air inlet of the fan in cold side (Fig. 3). By suctioning the air from the ambience through the filtration mask, where the temperature is lower than the human's exhaled air, the cooling effect will be improved in comparison to the internal air circulation. Moreover, the humidity of the ambient air is also lower than that directly from human breathing, avoiding

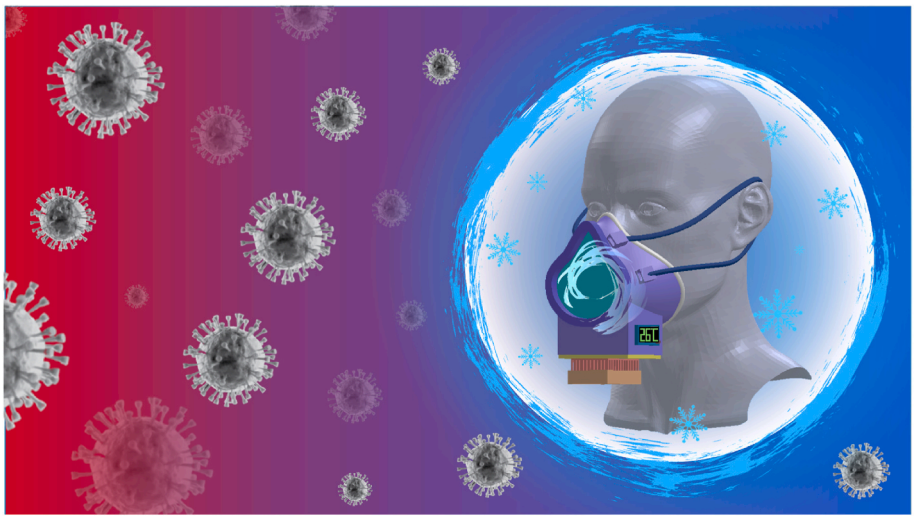

Fig. 1. Illustration of AC mask.

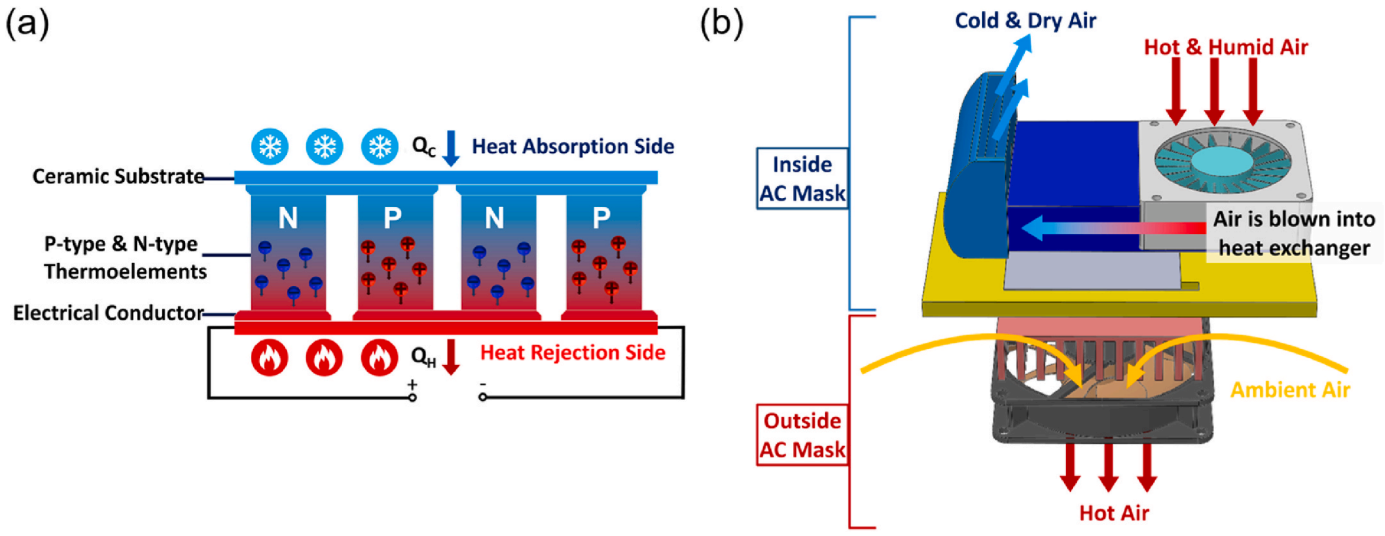

Fig. 2. Thermal management mechanism of AC Mask: (a) Peltier effect of the TE module; (b) thermal exchange and ventilation of the AC Mask.

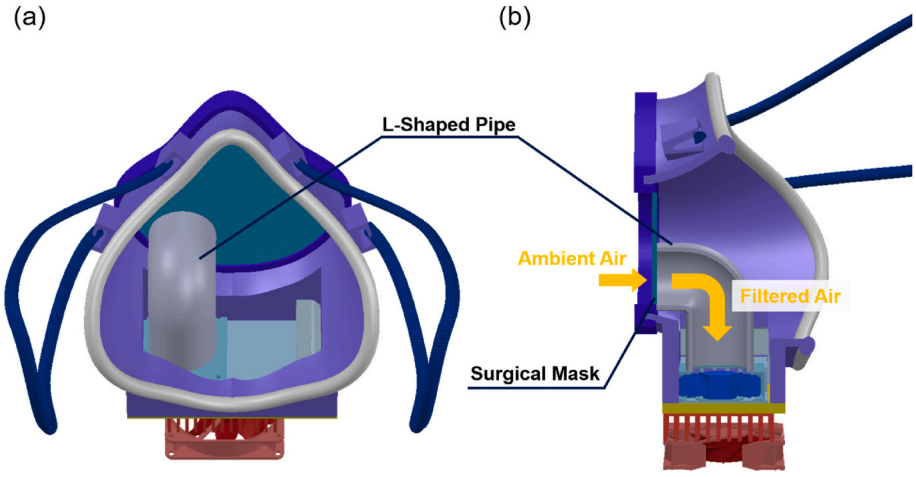

Fig. 3. (a) L-shaped pipe installation inside AC Mask; (b) Working principle of L-shaped pipe in AC Mask.

excessive moisture accumulation inside the facepiece.

2.2. Evaluation of thermal management

The thermoregulation based on the TE module and the fan speed affect the cooling performance and coolant flow of the AC Mask. Two types of heat exchangers were investigated (Fig. S3). The applied voltages of TE unit and fans in both cold and hot sides varied from 1V to 4V and 5V–11V, respectively. The row number of perforated holes on the copper sheet in the first type of heat exchanger were varied with 2 (Fig. S4a), 4 (Fig. S4b), and 8 (Fig. S4c) for each channel of the plate-fin heat sink. The heat exchanger with impermeable copper sheet was tested for guided air flow (Fig. S4d).

Steam tests were conducted to evaluate the cooling performance of the AC Mask based on the four different heat exchanger types under different voltages (Fig. S4). To simulate human breathing, heat and humidity sources were created by steam generation. The water vapor was produced by 250 ml boiled water, which was directed through a conical flask to supply warm moisture vapor within the AC Mask. Gore-Tex fabric was used to cover the conical flask, only allowing water vapor to pass from the boiled water to the AC Mask while maintaining the vapor temperature at 50 °C (to approximate a thermal microclimate at a high heat load) consistently during the test. The AC Mask was exposed to an environment in temperature set at (30 ± 1) °C with relative humidity (RH) at (60 ± 5)%. Polystyrene foam covering the conical flask was used to avoid heat loss to the surroundings. To better examine the cooling performance, the reduction in the apparent temperature (AT) was calculated based on the measurement of variations in temperature and humidity by a commercial temperature and humidity sensing system. The AT was equivalent to a human-perceived equivalent temperature, calculated by the formula:

$$AT = -2.653 + 0.994T + 0.0153T_d^2 \tag{1}$$

and

$$T_d = \frac{243.04\left(ln\,(RH) + \frac{17.625T}{243.04+T}\right)}{17.625 - ln\,(RH) - \frac{17.625T}{243.04+T}} \tag{2}$$

where AT is the apparent temperature, T is the dry-bulb temperature, T_d is the dew point temperature, and RH is the relative humidity [35,36]. The absolute humidity (AH) was used to indicate change in the amount of water vapor content in air inside the AC mask, and the formula for AH is given by Ref. [37]:

$$AH = \frac{6.112 \times e^{\left[\frac{17.67\times T}{T+243.5}\right]} \times RH \times 2.1674}{273.15 + T} \tag{3}$$

Both AT and AH were obtained based on the values of the measured temperature and RH inside the AC mask. The recorded data was smoothened by neighboring data points and the smoothing equal to a weighted average of them. In particular, Gaussian Function was employed to be the smoothing function, avoiding over high frequency oscillation.

The subject was exposed to an environment in temperature set at (30 ± 1) °C with RH at (60 ± 5)%. First, the AC Mask was worn by the subject for 10 min. Then the AC Mask was operated for 30 min and switched off until the temperature fell back to the initial state. A commercial temperature and humidity sensing system was used to measure the temperature and RH close to the nose area inside the AC Mask, and the thermocouples were used to monitor changes of the face skin temperature within throughout the whole human test, as shown in Fig. 4.

To obtain a better cooling performance analysis, a 3 M™ N95 Health Care Particulate Respirator and Surgical Mask (Product number 1860) was used to compare the temperature rise by 3 conditions: L-shaped pipe

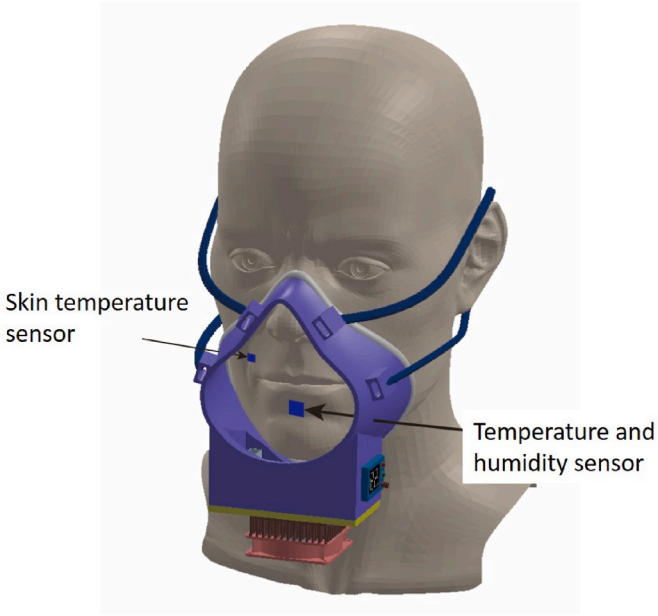

Fig. 4. Temperature and humidity sensors' location in human objective test.

installation, thermoregulation unit turned on and off. Based on the same location of the temperature and humidity sensors in Fig. 4, the temperature and AH were recorded right after the subject worn the AC Mask.

A total of 15 subjects (6 males and 9 females, 20–30) were recruited to wear the AC Mask in the human subjective test. The ambient condition was (32 ± 1) °C with RH at (63 ± 5)%. The total duration of the human subjective test was 20 min, with the TE unit off for 10 min and on for 10 min. Then the subjects were asked to provide feedback and complete the rating form (Tables S3–S5). Table S3 includes the ASHRAE seven-point scale and the Nicol five-point thermal preference scale that were used for Thermal Sensations Vote (TSV) and Thermal Preference (TP) [38]. Humidity Feeling (HF), Humidity Preference (HP) and Overall Comfort (OC) were also evaluted based on the subjects' perception [38,39] (see Tables S4 and S5). For the TSV, the ASHRAE seven-point scale was used, viz., cold (−3), cool (−2), slightly cool (−1), neutral (0), slightly warm (+1), warm (+2), and hot (+3). The subjects also indicated their TP, which was expressed in the Nicol five-point thermal preference scale, viz., much cooler (−2), a bit cooler (−1), no change (0), a bit warmer (+1), and much warmer (+2). Analogously, the HF and HP were measured based on the subjects' responses of humidity sensations. The OC was eventually rated to indicate the degree of comfort, viz., very comfortable (−3), moderately comfortable (−2), slightly comfortable (−1), neither comfortable nor uncomfortable (0), slightly uncomfortable (+1), moderately uncomfortable (+2), and very uncomfortable (+3).

Granuled calcium chloride ($CaCl_2$) with diameter of 1–2 mm was selected as desiccant materials for investigation of humidity management considering the great hygroscopic capacity [40]. $CaCl_{2(s)}$ is very unlikely to evaporate from the package due to its strong ionic bonding, avoiding diffusion into the human's respiratory system. The $CaCl_2$ has also been employed for medical usage [41]. The estimated moisture absorption amount is about 4 g–9 g of the moisture per unit gram of $CaCl_2$ under the mean temperature 31 °C and RH 85% [42]. Similar with the human objective test in the Temperature Control Management section, temperature and RH were recorded by the commercial temperature and humidity sensors after subjects wore the AC Mask with the 5g desiccants, which were firmly sealed in microporous packages. The 5-g desiccant pack was placed on the cold side of heat sink, as shown in Fig. 5 (left). In a different setting, 2 packs of desiccants with (2.50 ± 0.05) g each in average, were attached on the upper wall of the AC Mask

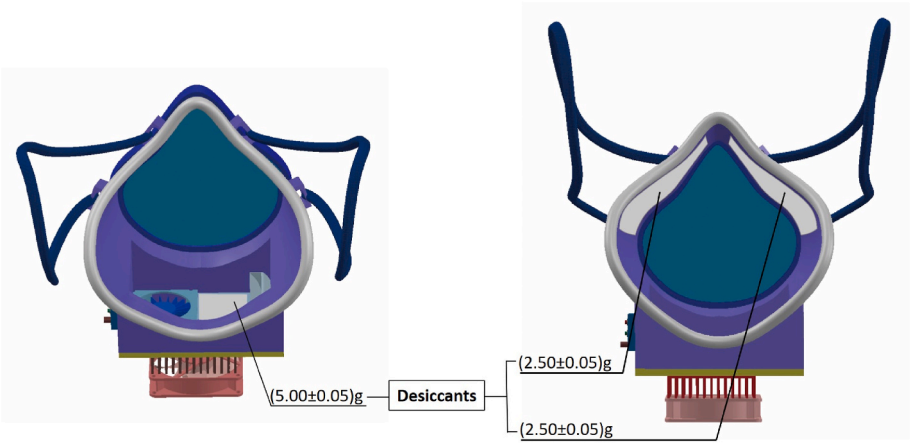

Fig. 5. Allocations of desiccants in AC Mask: 1 pack of (5.00 ± 0.05) g desiccant on the cold side of heat sink (left) and 2 packs of (2.50 ± 0.05) g in average per each pack of desiccant on the upper wall of the mask frame (right).

frame, as shown in Fig. 5 (right). In order to evaluate the effect of the $CaCl_2$ desiccants, 4 cases of experimental data were obtained from with and without thermoregulation unit operation, 1 and 2 pack(s) $CaCl_2$ allocations, respectively. The temperature and AH were measured right after the subject worn the AC Mask.

2.3. Filtration tests

To characterize the filtration performance of the proposed mask, a test setup has been built, as presented in Fig. S5. It consists of three parts: source of air flow with particles, a dummy wearing a mask, and a particle detector. The particles were generated by a smoke reactor. A fan was applied to drive the flowing particles to the mask. A particle detector was connected to the inside chamber of the mask through a silicon tube. In the test, two types of masks, i.e., a 3 M™ N95 Health Care Particulate Respirator and Surgical Mask (Product number 1860) and the proposed AC mask, were tested and compared.

2.4. Numerical simulation of cooling ventilation

A numerical simulation of the proposed AC Mask has been conducted using COMSOL 5.5 to reveal the thermal transport and temperature distribution. The boundary condition and generated meshes were presented in Fig. 6. The flow type inside the AC mask is determined by the Re number, which is expressed as:

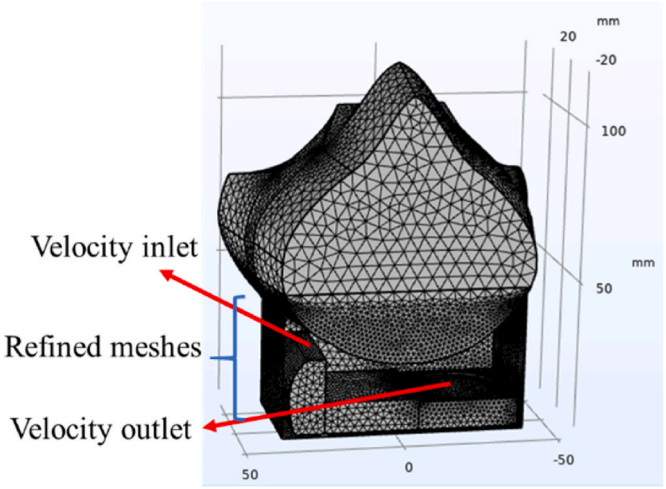

Fig. 6. The generated meshes of the mask with a refined meshes region.

$$Re = \frac{\rho V D}{\mu} \quad (4)$$

where ρ is the density of air (1.225 kg/m^3), V is the flowing velocity, μ is the dynamic viscosity of air (17.9x10^{-6} Pa s), D is the characterized length (44.8x10^{-3} m) which is defined as the hydraulic diameter of the cross section of AC mask (112x28 mm). It has been reported [43] that airflow velocities ranging from 0.25 m/s to 1 m/s are comfortable for human being. The flow velocity of the AC Mask fans can be adjusted to generate a comfortable airflow. The corresponding Re numbers have been calculated, which ranges from 769 to 3079, corresponding 0.25 m/s to 1 m/s, respectively. The actual flow velocity in the AC Mask is generally less than 1 m/s. Here, a Laminar flow model was applied for the simulation.

The non-isothermal flow was set as Multiphysics and the fluid material was air. A weakly compressible flow was set for the laminar flow under the pressure of 1 ATM. The inlet flowing air velocity was set to a comfortable value for human and the outlet boundary was a pressure outlet. The temperature for inflow air was 298.55 K. Initially, the velocity of the whole domain was 0 m/s and the temperature was 308.15 K with all-wall thermal insulation except for the inflow and outflow boundary. The mesh type was 3D-free tetrahedral with a minimum element size of 0.111 mm for the refined region and 1.48 mm for the basic region. The overall mesh number was 717,102, with an average element quality of 0.6603.

3. Results and discussion

3.1. Simulated breathing test and optimization of cooling effect

In the steam test, the change of AT was examined by different voltages applied to the TE unit and fans based on different structures of heat sink. The reduction in AT is shown in Fig. 7 and Fig. 8 on the basis of the 4 different heat sink types when the voltage of TE was fixed at 3V. In all cases, the values of AT became constant within 10 min. In particular, the AT was significantly reduced, ranging from 15 °C based on Heat Sink A to over 30 °C based on Heat Sink D with the fan voltage of 9V on the hot side. It is also noted that, based on Heat Sinks A, B and C, the cooling performance of the AC Mask was maximized when the voltage for the fan was set at 7V, but that for Heat Sink D shifted to 9V. The optimal voltage applied to the fan on the hot side exists, possibly because the lower voltage limited the air flow for heat exchange and the too high voltage imposed intrinsic heat to the AC Mask. Among these heat sinks, Heat Sink D revealed the best cooling performance based on according to the temperature reduction.

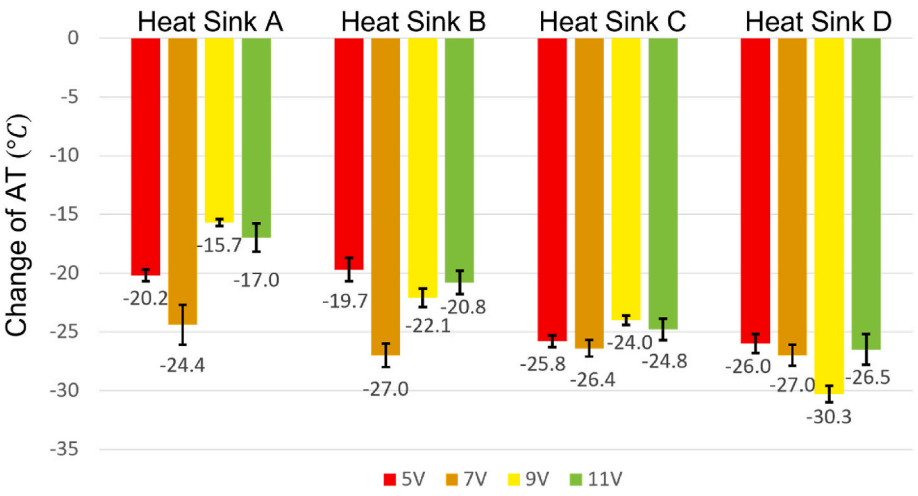

Fig. 7. Change of AT on the basis of different voltages applied to the fan in the cold side when the voltage of TE is fixed at 3V.

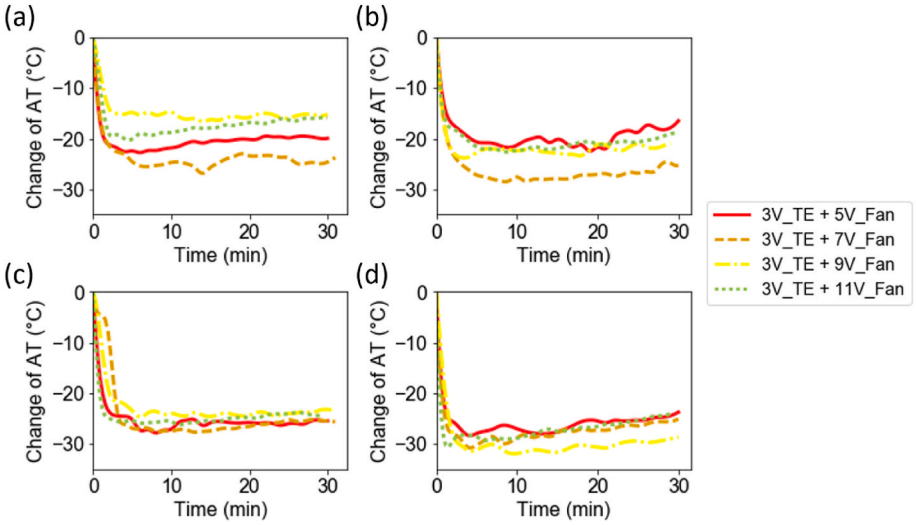

Fig. 8. Effects of the voltage applied to the fan in the cold side on the AT in the AC Mask under a constant TE voltage of 3V with (a) Heat sink A, (b) Heat sink B, (c) Heat sink C and (d) Heat sink D.

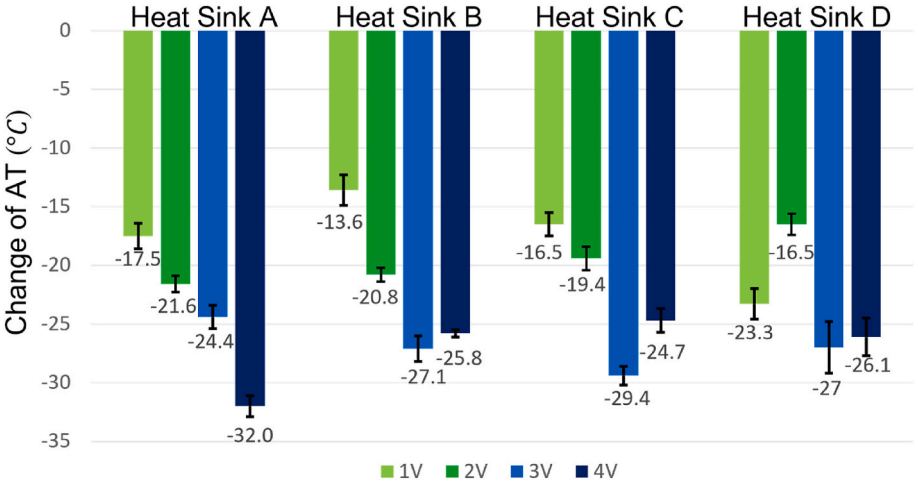

Fig. 9. Change of AT on the basis of different voltages applied to the TE when the voltage applied to the fan is fixed at 7V.

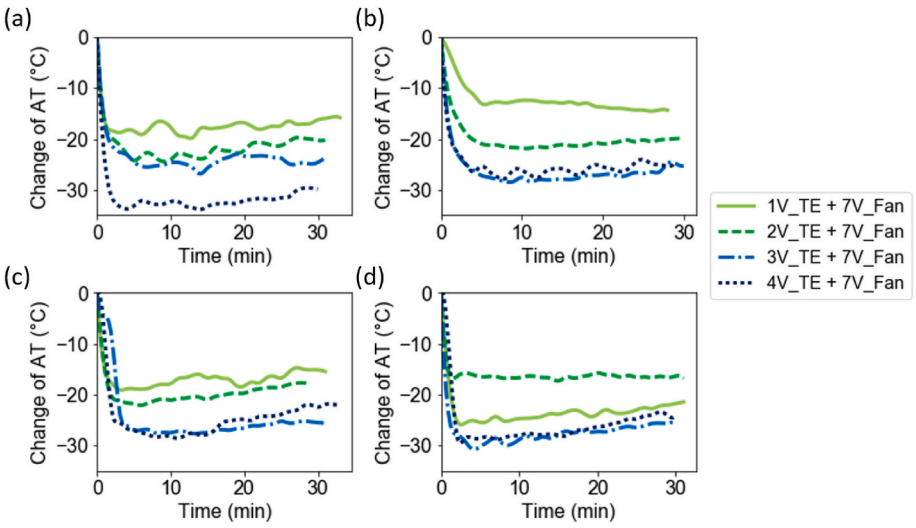

Fig. 10. Effects of the voltage applied to the TE on the AT in the AC Mask under a constant fan voltage on both of the cold and hot sides at 7V, with (a) Heat sink A, (b) Heat sink B, (c) Heat sink C and (d) Heat sink D.

Fig. 9 and Fig. 10 demonstrate the changes of AT with different voltages applied to the TE under the fixed voltage applied to the fans on both cold and hot sides at 7V, on the basis of the 4 different heat sink types. The test process was the same to that in Fig. 7. It is shown that the reduction of AT is 13 °*C* with Heat Sink B when the TE voltage is 1V to over 30 °*C* with when the TE voltage is 4V. In general, a higher voltage applied to the TE led to superior cooling performance for all heat sinks. However, it is interesting to note that the AT was reduced when the voltage applied on the TE varied from 3V to 4V, indicating that a possible optimal voltage exists for maximum cooling performance.

To better visualize the effects of the voltages applied to both TE and fans and explore the optimization of cooling performance, the change of AT was examined with variations in the voltages applied to TE and fans on both hot and cold sides on the basis of Heat Sink B in the AC Mask (Fig. 11). We found that the trend of reduction in both temperature and AT increased with the TE voltage and the fan voltage. However, under a constant fan voltage, e.g., 7V, the maximum temperature reduction was obtained when the TE voltage was close to 3.5V in Fig. 11a. The optimal condition was possibly attributed to increase of the cooling effect with voltage, but the excessive heat was generated with a high voltage. Similarly, a local optimum condition was found for the AT in Fig. 11b. The maximum cooling effect was found when the voltages were close to the upper values in Fig. 10, but the high-power consumption would limit the application of this portable system. Based on the Peltier effect, the greater cooling power can be generated with the increasing voltage. However, the thermoelectric unit has an intrinsic maximum Coefficient of Performance (COP) at a certain current or voltage, which depends on the design of the thermoregulation unit including the heat dissipation efficiency [44]. The continuously increasing voltage will lead to extra heat inside the thermoelectric module and consequently reduce the COP. With the optimized power management, the enhanced cooling effect can be obtained at a lower energy consumption for longer working duration. Thus, it is critically valuable to find the local optimization for enhanced thermal comfort when the voltage and power consumption are sufficiently low.

The AC Mask allows adjustment of temperature and AT towards users' requirements. It is shown in Fig. 12 that both temperature and AT vary with the voltage applied to the TE unit from 1V to 3V and then conversely, in every 10-min interval, with the voltage applied to the fans in both hot and cold sides fixed at 7V on the basis of Heat Sink B in the AC Mask. Therefore, the temperature and AT could be well regulated, consistent with a temperature- or humidity-responsive control system in future work.

3.2. *Numerical simulation of thermal ventilation*

Fig. 13 presents the temperature distribution with a streamline of the AC mask with the wind guided tunnel at various states. Streamline shows that a high-velocity region is in a band-shape along the flowing direction of inlet air. The band-shape low-temperature region is overlapped with the high-velocity region (Fig. 13c). The wind-guided tunnel is effective since the fresh flowing air is guided to the central zone (close to the nose). The cool air with a temperature of 25 °C is directed to the nose zone. The inside temperature of the mask is majorly reduced from

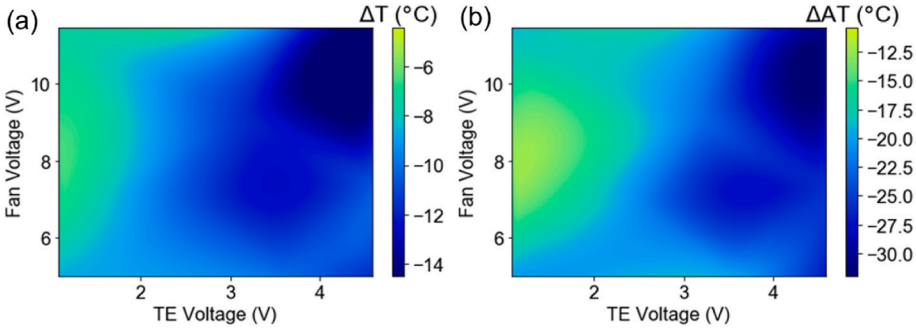

Fig. 11. (a) Temperature change and (b) AT with variations in the voltages applied to TE and fans on both of the hot and cold sides on the basis of Heat Sink B in the AC Mask.

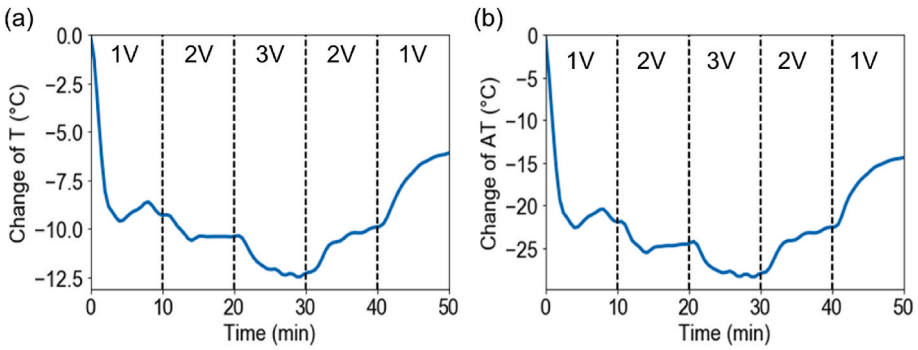

Fig. 12. Variations of (a) Temperature and (b) AT with the voltage applied to the TE unit from 1V to 3V and then reversely with the voltage applied to the fans in both hot and cold sides fixed at 7V on the basis of Heat Sink B in the AC Mask.

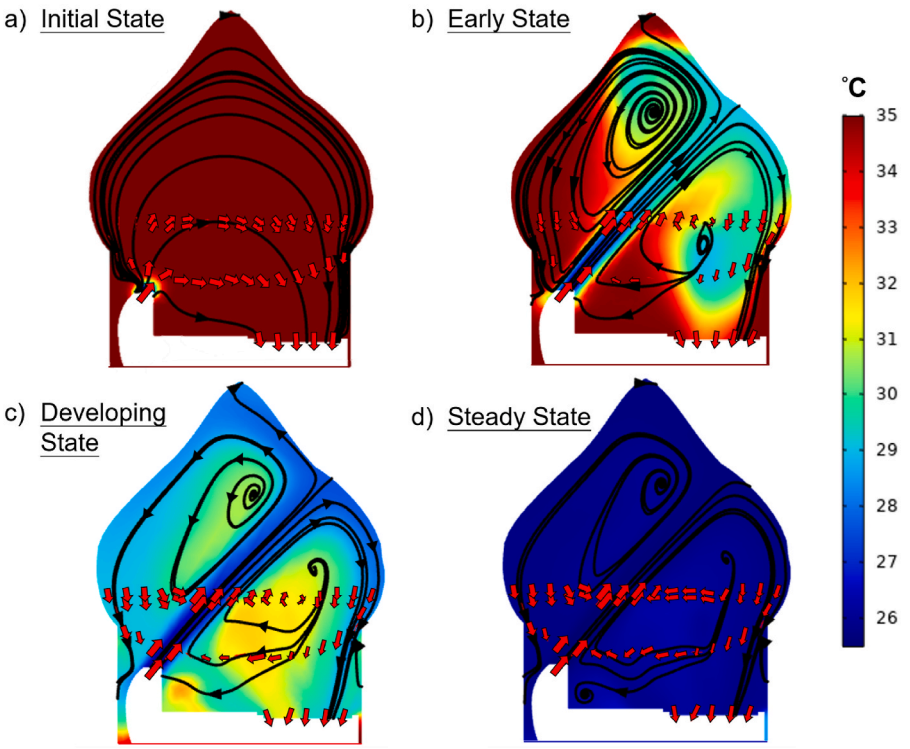

Fig. 13. The temperature field combined with the streamline of the AC mask at the time of (a) Initial State, (b) Early State, (c) Developing State, and (d) Steady State.

35 °C (Fig. 13a) to (25–27) °C (Fig. 13d), indicating the effectiveness of the AC cooling. Besides, the unevenly distributed temperature field of flowing air will make the person feel uncomfortable [45]. In the proposed AC mask, the temperature field is eventually uniform (Fig. 13d), which increases the thermal comfort as well. The streamline also presents that the air flow is separated into two directions after it reaches the sidewall, which promotes the convection inside the chamber.

3.3. Human tests and thermal and moisture management

It is critically important to conduct human trial test to examine the performance of AC Mask for actual applications. Heat sink B and Heat sink D, which had the greatest cooling performance among the four different types of heat sink were chosen for the human tests by setting the voltages applied to TE and the fans targeting at 3V and 9V, respectively. The environmental temperature and absolute humidity remained at $(30 \pm 1)\,^{\circ}C$ and $(15.8 \pm 0.3)\,g/m^3$.

During the testing, the voltage and current output of fans and TE module recorded by oscilloscope (KEYSIGHT 34470 A), as shown in Fig. 14. The total average power consumed for the human objective test was $(7.03 \pm 0.18)\,W$. The sound of a working AC Mask comes from the tiny fans. We measured the sound pressure level (SPL), which was equal to 49.5 dB (equivlenet to the sound in a quiet library [46]).

After the AC Mask with Heat Sink B was put on by the subjects, the temperature of the mask microclimate dropped by $(1.82 \pm 0.05)\,^{\circ}C$ with the TE unit turned on, as seen in Fig. 15a. As well, the value of AH dropped by $(3.19 \pm 0.39)\,g/kg$ with great reduction in humidity and the values of AT in Fig. 15c decreased by $(3.59 \pm 0.23)\,^{\circ}C$. The AC Mask allows adjustment of temperature and AT towards users' requirements. It is shown in Figs. 15a and c that both temperature and AT vary with the voltage applied to the TE unit when the voltage applied to the fans in both hot and cold sides is fixed at 9V on the basis of Heat Sink B in the AC Mask. By varying the voltage across TE unit, the temperature and AT could be well regulated, consistent with a temperature- or humidity-responsive control system in future work. Meanwhile, the skin temperature decreased by $(1.17 \pm 0.11)\,^{\circ}C$ as shown in Fig. 15d. The decreased AH helps to reduce the hot sensation or AT substantially, improving thermal comfort and ease of breath for the wearers.

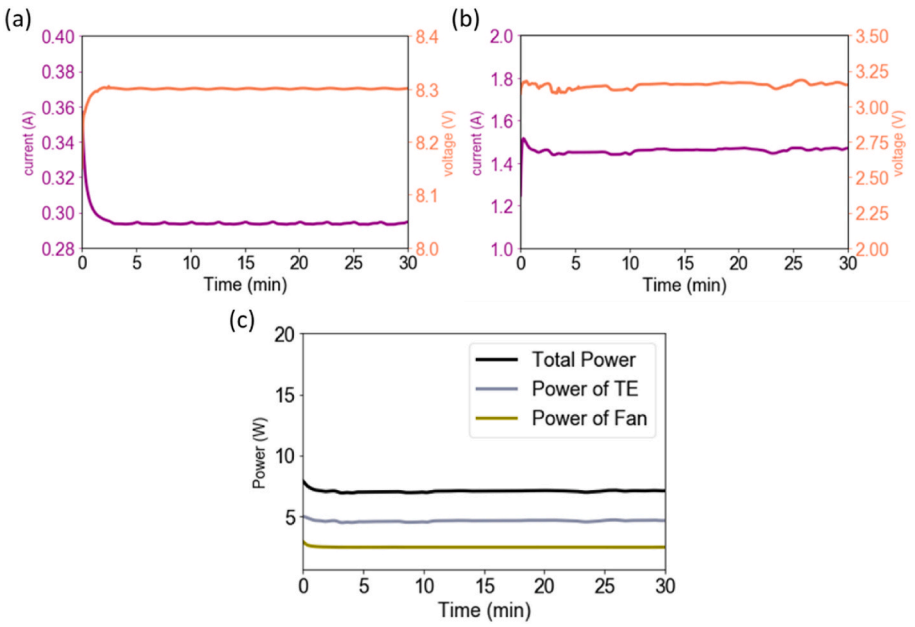

Fig. 14. Voltage and current versus time supplied to (a) Fans in both heat supply and rejection sides, (b) TE unit. (c) The power supplied for the AC Mask.

The AC Mask on the basis of Heat Sink D (Fig. 15e–h) was also evaluated following the same procedure in Fig. 15a–d. It is noted that the reduction in the temperature and AH is $(2.57 \pm 0.23)\,^{\circ}C$ and $(3.26 \pm 0.74)\,g/kg$, respectively, and the drop in AT is close to $(4.41 \pm 0.57)\,^{\circ}C$, consisting with the cooling performance demonstrated in the steam test. The greater drop in temperature inside the AC Mask resulted from the greater forced air flow guided by the 3D printed tunnel towards the subject's nose and mouth.

According to the evaluated results, Heat Sink D was chosen as the experimental setup for the cooling performance comparison due to a greater temperature reduction in the human objective test. The AH and AT difference has been obtained after the subtraction of ambient temperature and humidity during the 30-min mask wearing experiment (Fig. 16 and Fig. 17). The temperature inside the mask increased slightly by $(5.49 \pm 0.13)\,^{\circ}C$ when the subject was wearing AC mask with TE and fan at 3V and 9V respectively, which is 26% reduced after comparing with the temperature increment ($(7.43 \pm 0.44)\,^{\circ}C$)with the N95 mask. Particularly, $(3.05 \pm 0.20)\,^{\circ}C$ was increased with an L-shaped pipe installation in AC Mask, showing that the cooling performance was improved significantly by air suctioning from ambience than directly from the human exhalation. In short, the reductions in the apparent microclimate temperature and the humidity by around 3.5 °C (Figs. 17a) and 50% (Fig. 17b), respectively, have been achieved under a low voltage.

Similarly, the AC Mask including Heat Sink D was applied for evaluation of the humidity management. The humidity reduction contributed by $CaCl_2$ was recorded based on the comparison in temperature, AH and AT, under fixed voltage supplied to TE and fans at 3V and 9V, respectively, as shown in Fig. 18 and Fig. 19. After the AC Maks worked for 30 min, the weight of 1 pack and 2 packs $CaCl_2$ was increased by (0.50 ± 0.05) g and(0.90 ± 0.05) g, respectively, corresponding to the moisture absorption amounts by $CaCl_2$. Fig. 18 shows the results in change of temperature, AH and AT under 4 operation settings. It was found in Fig. 19a that the rate of temperature increased was lower with the aid of thermoregulation unit, showing that the TE unit could decrease the heat gained inside the mask. Figs. 19b and c showed that the overall changes of AH and AT were lower after $CaCl_2$ was added. The heat sink surface temperature was lower than the dew point, indicating that the vapor pressure was greater than the corresponding saturated pressure of the surface. Hence, the moisture in gas phase condensed into liquid phase and the humidity was reduced accordingly. Owing to the heat releasing when $CaCl_2$ moisture absorption, more heat was released with higher moisture absorption amounts. Therefore, the change of temperature was slightly higher in 2 packs of $CaCl_2$ than the other cases.

3.4. Subjective evaluation

The human subjective test was carried based on five significant factors, including Thermal Sensations Vote (TSV), Thermal Preference (TP), Humidity Feeling (HF), Humidity Preference (HP) and Overall Comfort (OC). The rating of cooling performance was conducted with the N95 mask and the AC Mask on the basis of Heat Sink D. As seen in Fig. 20 and Table S6, the AC Mask improved the dryness, coolness and the overall comfort of the subjects. As well, the AC mask based on programmable design of 3D printed frames fitted most of the subjects. The results of TP and OC with the AC Mask were found to be much better than with the N95 mask, indicating good thermal management performance and wear comfort.

4. Conclusion

Based on the experimental and numerical invstigation conducted in this paper, the following conclusions can be drawn:

(1) Based on the human trial, a reduction in the microclimate temperature and user's face temperature at 2.6 °C and 1.1 °C, respectively, has been achieved under a low power consumption at 7.03 W.
(2) The decrease in the apparent temperature, that equivalent perceived by humans by the combined effects of air temperature, RH and wind speed, is over 4 °C under human trial and 30 °C under the steam test. The moisture content in terms of RH has also been reduced from 82% to 75%.
(3) The optimal operation conditions with maximum temperature reduction (e.g., 18 °C) against variations in the applied voltage have been derived.
(4) In the future work, the AC Mask will be improved with reduced weight and power consumption. The slight condensation, which is generated with the reduction in humidity of the mask microclimate, will be transferred and absorbed by highly wicking

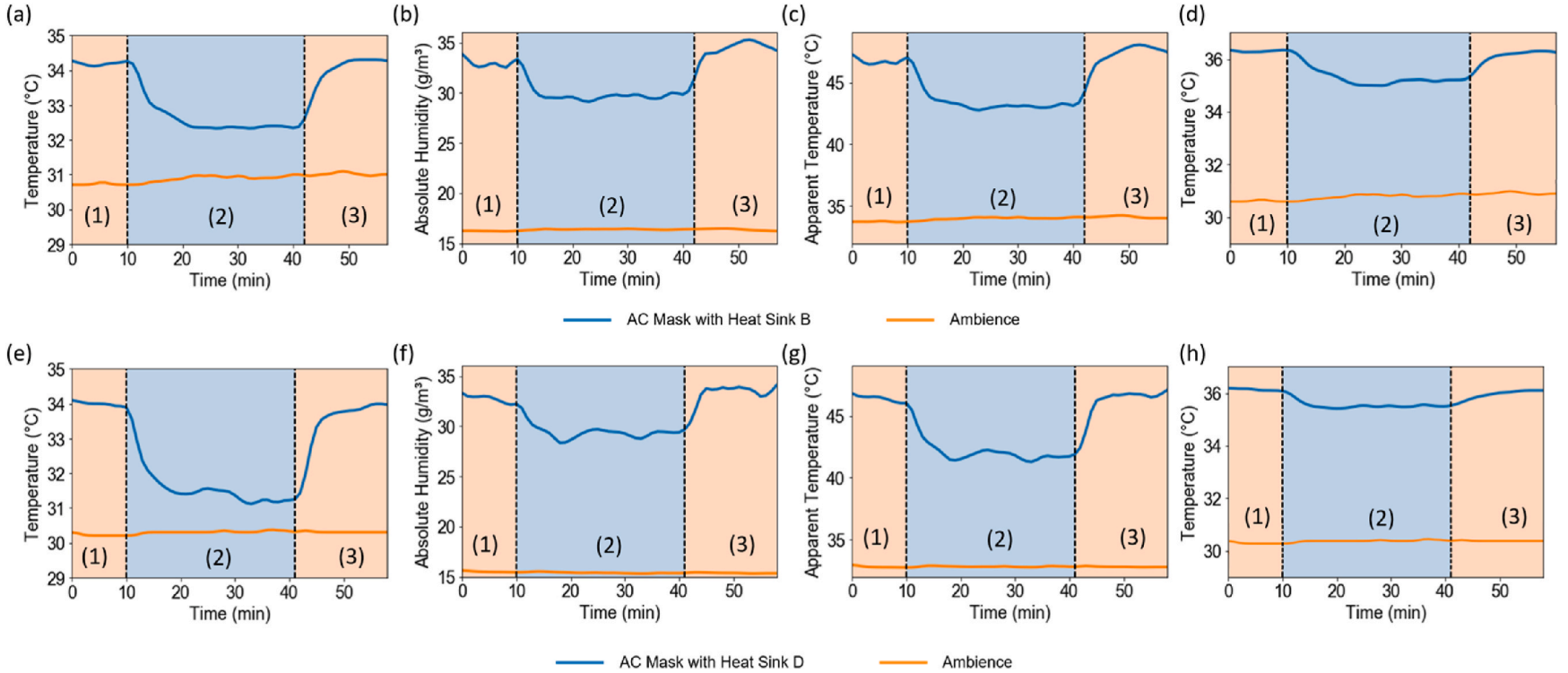

Fig. 15. Performance evaluation of AC Mask when (1) AC Mask was put on by the user; (2) the TE unit turned on with the TE voltage at 3V and the fan voltages in both hot and cold sides at 9V; (3) the TE unit turned off, by measuring (a) microclimate temperature, (b) absolute humidity, (c) apparent temperature, and (d) skin temperature on the basis of Heat Sink B; (e) microclimate temperature, (f) absolute humidity, (g) apparent temperature and (h) skin temperature on the basis of Heat Sink D.

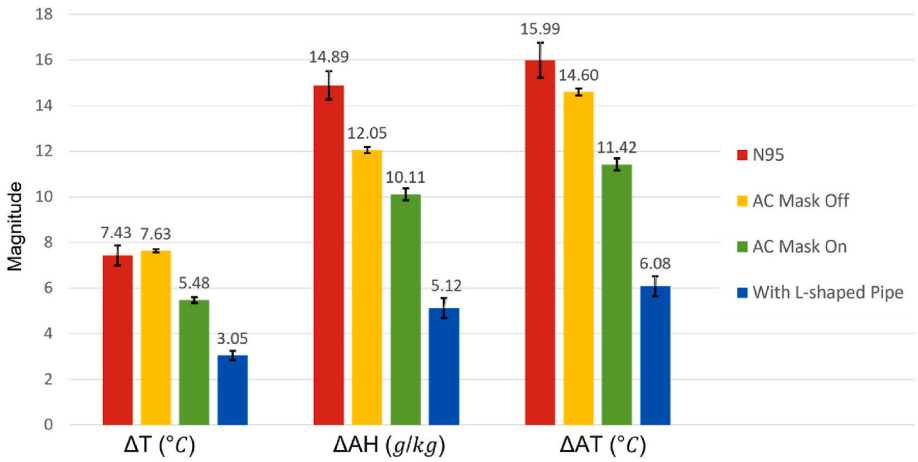

Fig. 16. Change of temperature, AH and AT on the basis of 4 different settings under a fixed voltage applied to the TE and the fan at 3V and 9V, respectively.

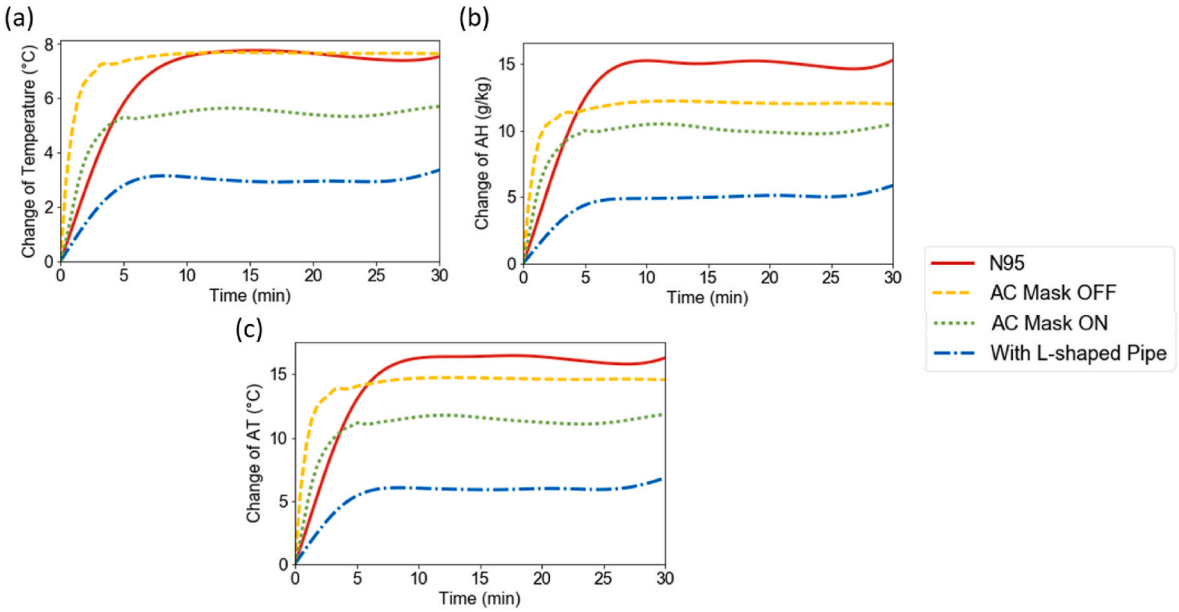

Fig. 17. Change of (a) temperature, (b) AH and (c) AT on the basis of 4 different settings under fixed voltage applied to the TE and fan at 3V and 9V respectively.

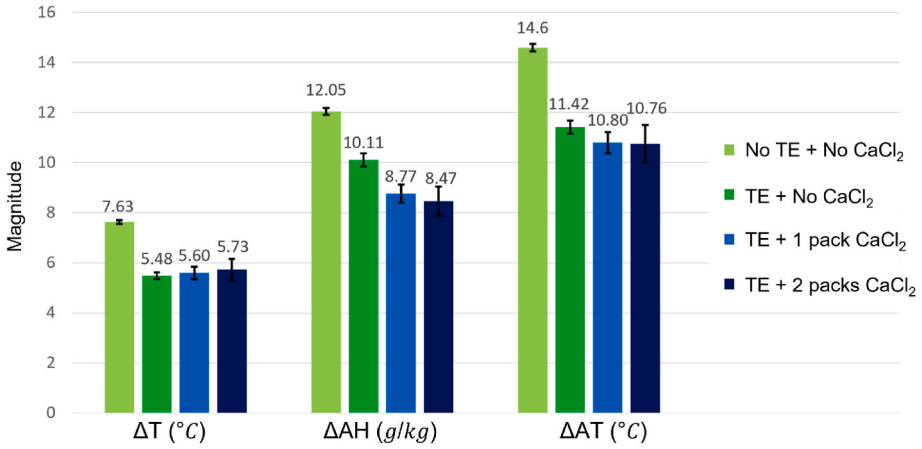

Fig. 18. Change of temperature, AH and AT on the basis of 4 different AC Mask operating settings under a fixed voltage applied to the TE and the fan at 3V and 9V, respectively.

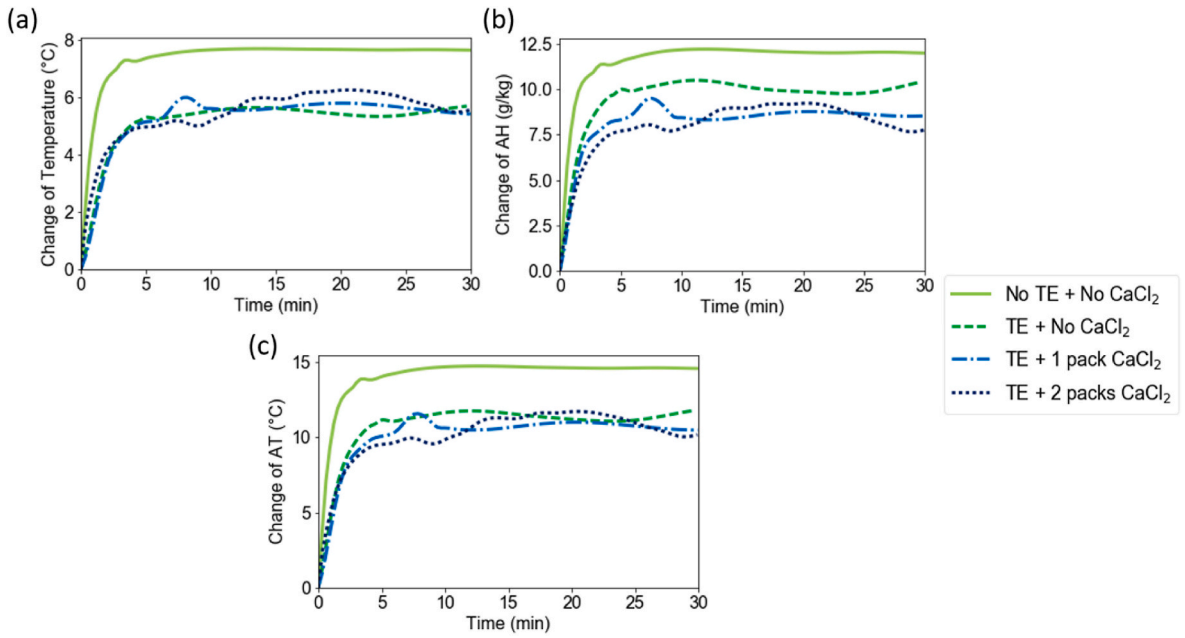

Fig. 19. Change of (a) temperature, (b) AH and (c) AT on the basis of 4 different AC Mask operating settings under fixed voltage applied to the TE and fan at 3V and 9V respectively.

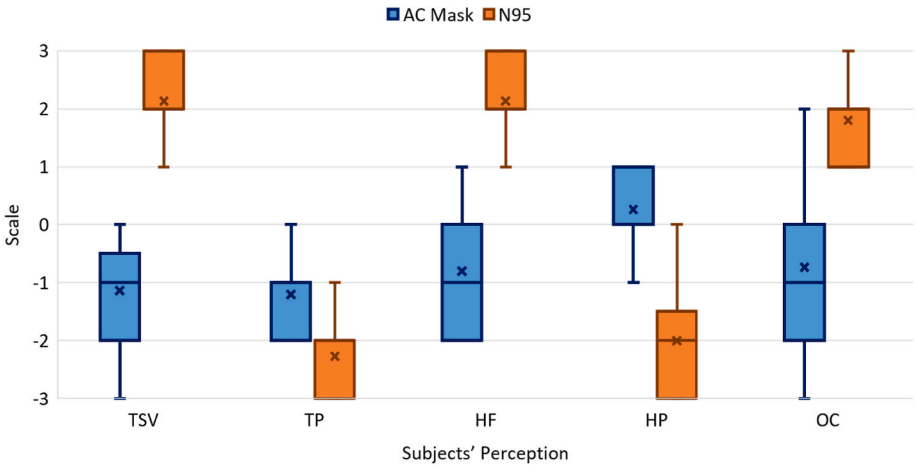

Fig. 20. Summary of the human subjective test.

materials. By switching the voltage, the warming effect with be investigated experimentally and theoretically.

It has been shown that the facemask wearing hiders transpiration and cooling of the skin, which leads to the increase in skin temperature and human perception discomfort significantly [47]. With the proof-of-concept AC Mask prototype, the thermal comfort was improved with 2.6 °C dropped inside the mask (Fig. 15d) as the face was the most thermo-sensitive part with high density of thermoreceptors for human thermoregulation [48,49]. As the thermal comfort was a state of mind [50], human subjective test indicated that the thermal management of AC Mask can achieve the cooling performance well. The cooling performance in the AC mask was dependent on the efficiency of heat transfer on TE module, which can be further enhanced by employing a higher figure-of-merit (ZT) TE materials [51,52]. Moreover, in order to take advantages of the latest inventions on surgical masks, AC Mask was designed as an integration with surgical masks and AC Mask frame to consolidate the AC Mask filtration performance. For example, the laser-induced graphene (LIG) mask can be unitized in AC Mask to improve the inhibition rate of bacteria viability which was adhesive on the outer surface of surgical mask [53]. The total weight of AC Mask is 284g, including the battery (i.e., a 5000 mAh lightweight power bank at 94g) placed in the pocket. In regard to the weight on the wearer's head, the AC Mask frame (190g) is 6% heavier than 3 M™ half mask HF-800 Series (182g) [54], 45.6% lighter than 3 M™ 6000 series half mask respirators including filters (355g) [55], and 38% lighter than Xupermask (313g) [56], a newly commercialized functional facemask. With the future development of high-performance miniaturized batteries, the power unit could be directly attached to the mask frame.

Declaration of competing interest

The authors declare that they have no known competing financial interests or personal relationships that could have appeared to influence the work reported in this paper.

Acknowledgements

Dr. Shou acknowledges the support from The Hong Kong Polytechnic University (Project No: BE1F and UAMA), Research Grants Council of Hong Kong (Project No: PolyU 252029/19E), and Innovation and Technology Fund of Hong Kong (Project No: ITS/093/19). The authors are also grateful to Magnum Chau for the source of the human head model.

Appendix A. Supplementary data

Supplementary data to this article can be found online at https://doi.org/10.1016/j.buildenv.2021.108236.

References

[1] T.N.S.a.H. Niosh, Use of respirators and surgical masks for protection, AORN J. (2018). Elsevier.
[2] L.R. Goldfrank, C.T. Liverman, Institute of Medicine Committee on Personal Protective Equipment for Healthcare Workers during an Influenza. Preparing for an Influenza Pandemic: Personal Protective Equipment for Healthcare Workers, National Academies Press, Washington, D.C., 2008. Washington, D.C.
[3] P. Harber, S. Barnhart, B.A. Boehlecke, W.S. Beckett, T. Gerrity, M.A. Mcdiarmid, E. Nardbell, L. Repsher, L. Brousseau, T.K. Hodous, M.J. Utell, Respiratory protection guidelines March Respiratory protection guidelines. This official statement of the American Thoracic Society was adopted by the ATS Board of Directors, March 1996, Am. J. Respir. Crit. Care Med. 4 (1996) 1153–1165.
[4] N.H. Leung, D.K. Chu, E.Y. Shiu, K.-H. Chan, J.J. McDevitt, B.J. Hau, H.-L. Yen, Y. Li, D.K. Ip, J. Peiris, Respiratory virus shedding in exhaled breath and efficacy of face masks, Nat. Med. 26 (5) (2020) 676–680.
[5] J. Bedford, D. Enria, J. Giesecke, D.L. Heymann, C. Ihekweazu, G. Kobinger, H. C. Lane, Z. Memish, M.-d. Oh, A. Schuchat, COVID-19: towards controlling of a pandemic, Lancet 395 (10229) (2020) 1015–1018.
[6] S. Feng, C. Shen, N. Xia, W. Song, M. Fan, B.J. Cowling, Rational use of face masks in the COVID-19 pandemic, Lancet Respir. Med. 8 (5) (2020) 434–436.
[7] K. Everington, Masks Mandatory on Taiwan Trains, Intercity Buses Starting Today, 2020. Taiwan News.
[8] C.C. Leung, T.H. Lam, K.K. Cheng, Mass masking in the COVID-19 epidemic: people need guidance, Lancet 395 (10228) (2020) 945.
[9] T. Greenhalgh, M.B. Schmid, T. Czypionka, D. Bassler, L. Gruer, Thermal sensation of the body as influenced by the thermal microclimate in a face mask, Ergonomics (2020) 369.
[10] R. Zhang, Y. Li, A.L. Zhang, Y. Wang, J.M. Molina, Identifying airborne transmission as the dominant route for the spread of COVID-19, Natl. Acad. Sci. (2020).
[11] T.W. Reader, U.W. Bowen Jr., Face Masks Including a Spunbonded/meltblown/spunbonded Laminate, Google Patents, 1999.
[12] R. Nielsen, L.G. Berglund, A.R. Gwosdow, A. Dubois, Thermal sensation of the body as influenced by the thermal microclimate in a face mask, Ergonomics 30 (12) (1987) 1689–1703.
[13] J. Meyer, M. Hery, J. Herrault, G. Hubert, D. Francois, G. Hecht, M. Villa, Field study of subjective assessment of negative pressure half-masks. Influence of the work conditions on comfort and efficiency, Appl. Ergon. 28 (5–6) (1997) 331–338.
[14] Y. Li, H. Tokura, Y. Guo, A. Wong, T. Wong, J. Chung, E. Newton, Effects of wearing N95 and surgical facemasks on heart rate, Int. Arch. Occup. Environ. Health 78 (6) (2005) 501–509.
[15] C. Godoy, D. Thomas, Technology, influence of relative humidity on HEPA filters during and after loading with soot particles, Aerosol Sci. Tech. (2020) 1–12.
[16] M. Kaywhite, T.K. Hodous, M. Vercruyssen, Effects of thermal environment and chemical protective clothing on work tolerance, physiological responses, and subjective ratings, Ergonomics 34 (4) (1991) 445–457.
[17] M. Morabito, A. Messeri, A. Crisci, L. Pratali, M. Bonafede, A. Marinaccio, Heat warning and public and workers' health at the time of COVID-19 pandemic, Sci. Total Environ. 738 (2020) 140347.
[18] B.V. Shenal, L.J. Radonovich Jr., J. Cheng, M. Hodgson, B.S. Bender, Discomfort and exertion associated with prolonged wear of respiratory protection in a health care setting, J. Occup. Environ. Hyg. 9 (1) (2012) 59–64.
[19] A.S. Baig, C. Knapp, A.E. Eagan, L.J. Radonovich Jr., Health care workers' views about respirator use and features that should be Included in the next generation of respirators, Am. J. Infect. Control 38 (1) (2010) 18–25.
[20] U.S.F.a.D. Administration, N95 Respirators, Surgical Masks, and Face Masks, 2020.
[21] M.E. Gosch, R.E. Shaffer, A.E. Eagan, R.J. Roberge, V.J. Davey, L.J. Radonovich Jr., Am. J. Infect. Control 41 (12) (2013) 1224–1230.
[22] D.A. Japuntich, N.V. McCullough, Respirator that Includes an Integral Filter Element, an Exhalation Valve, and Impactor Element, Google Patents, 2002.
[23] R.J. Roberge, Are exhalation valves on N95 filtering facepiece respirators beneficial at low-moderate work rates: an overview, J. Occup. Environ. Hyg. 9 (11) (2012) 617–623.
[24] S. Verma, M. Dhanak, J. Frankenfield, Visualizing droplet dispersal for face shields and masks with exhalation valves, Phys. Fluids 32 (9) (2020), 091701.
[25] P.S. Potnis, C.K. Nash, E.C. Steindorf, A.Y. Houde, J.D. Hurdle, Face Mask Having Improved Comfort through Cooling of Microclimate through Use of a Phase Change Material, Google Patents, 2019.
[26] J.M. Waligora, E. Michel, Application of conductive cooling for working men in a thermally isolated environment, Aero. Med. 39 (5) (1968) 485–487.
[27] T.D. Chinevere, B.S. Cadarette, D.A. Goodman, B.R. Ely, S.N. Cheuvront, M. N. Sawka, Efficacy of body ventilation system for reducing strain in warm and hot climates, Eur. J. Appl. Physiol. 103 (3) (2008) 307–314.
[28] X. Xu, J. Gonzalez, Determination of the cooling capacity for body ventilation system, Eur. J. Appl. Physiol. 111 (12) (2011) 3155–3160.
[29] W. Yi, Y. Zhao, A.P.C. Chan, Evaluation of the ventilation unit for personal cooling system, Int. J. Ind. Ergon. 58 (2017) 62–68 (PCS).
[30] Z. Kang, X. Wan, F. Wang, A new hybrid personal cooling system (HPCS) incorporating insulation pads for thermal comfort management: Experimental validation and parametric study, Build. Environ. 145 (2018) 276–289.
[31] W. Song, F. Wang, F. Wei, Environment, Hybrid cooling clothing to improve thermal comfort of office workers in a hot indoor environment, Build. Environ. 100 (2016) 92–101.
[32] D. Zhao, X. Lu, T. Fan, Y.S. Wu, L. Lou, Q. Wang, J. Fan, R. Yang, Personal thermal management using portable thermoelectrics for potential building energy saving, Appl. Energy 218 (2018) 282–291.
[33] L. Lou, D. Shou, H. Park, D. Zhao, Y.S. Wu, X. Hui, R. Yang, E.C. Kan, J. Fan, Buildings, thermoelectric air conditioning undergarment for personal thermal management and HVAC energy saving, Energy Build. (2020) 110374.
[34] J. Lunt, Large-scale production, properties and commercial applications of polylactic acid polymers, Polym. Degrad. Stabil. 59 (1–3) (1998) 145–152.
[35] M.G. Lawrence, The relationship between relative humidity and the dewpoint temperature in moist air: A simple conversion and applications, Bull. Amer. 86 (2) (2005) 225–234.
[36] R. Cao, Y. Wang, J. Huang, J. He, P. Ponsawansong, J. Jin, Z. Xu, T. Yang, X. Pan, T. Prapamontol, G. Li, The mortality effect of apparent temperature: a multi-city study in Asia, Int. J. Environ. Res. Publ. Health 18 (9) (2021) 4675.
[37] Y.A. Cengel, Introduction to Thermodynamics and Heat Transfer, McGraw-Hill, New York, 1997.
[38] S.A. Damiati, S.A. Zaki, H.B. Rijal, S.J. Wonorahardjo, Environment, Field study on adaptive thermal comfort in office buildings in Malaysia, Indonesia, Singapore, and Japan during hot and humid season, Build. Environ. 109 (2016) 208–223.
[39] M. Indraganti, R. Ooka, H.B. Rijal, Thermal comfort in offices in summer: findings from a field study under the 'setsuden'conditions in Tokyo, Build. Environ. 61 (2013) 114–132.
[40] X. Zhang, K. Sumathy, Y. Dai, R. Wang, Parametric study on the silica gel–calcium chloride composite desiccant rotary wheel employing fractal BET adsorption isotherm, Int. J. Energy Res. 29 (1) (2005) 37–51.
[41] V. PL, R.I. Slepova, I.F. Satave, Inhalation of calcium chloride aerosols in complex therapy of pulmonary tuberculosis, Kazanskii Meditsinskii Zhurnal 4 (1962) 7–9.
[42] D.E. Garrett, Handbook of Lithium and Natural Calcium Chloride, Elsevier, 2004.
[43] R.S. Spain, Energy Savings in Buildings Using Fans and Allowing Floating Temperatures in Rooms, Texas A&M University, 1985.
[44] H.S. Lee, Thermal Design: Heat Sinks, Thermoelectrics, Heat Pipes, Compact Heat Exchangers, and Solar Cells, John Wiley & Sons, 2010.
[45] M. Aliahmadipour, M. Abdolzadeh, K. Lari, Air flow simulation of HVAC system in compartment of a passenger coach, Appl. Therm. Eng. 123 (2017) 973–990.
[46] O. Oyedepo, R. Ekom, K.A. Ajala, Analysis of traffic noise along oyemekun-oba-adesida road akure ondo state nigeria, J. Eng. Sci. Technol. 6 (2013) 72–77.
[47] I. Laird, R. Goldsmith, R. Pack, A. Vitalis, The effect on heart rate and facial skin temperature of wearing respiratory protection at work, Ann. Occup. Hyg. 46 (2) (2002) 143–148.
[48] J.C.S.K. CHoo, Research, Temperature sensitivity of the body surface over the life span, Somatosens. Mot. Res. 15 (1) (1998) 13–28.
[49] M. Nakamura, T. Yoda, L.I. Crawshaw, S. Yasuhara, Y. Saito, M. Kasuga, K. Nagashima, K. Kanosue, Regional differences in temperature sensation and thermal comfort in humans, J. Appl. Physiol. 105 (6) (2008) 1897–1906.
[50] N. Djongyang, R. Tchinda, D. Njomo, Thermal comfort: a review paper, Renew. Sustain. Energy Rev. 14 (9) (2010) 2626–2640.
[51] L. Bell, Cooling, heating, generating power, and recovering waste heat with thermoelectric systems, Science 321 (5895) (2008) 1457–1461.
[52] X. Shi, L. Chen, C. Uher, Recent advances in high-performance bulk thermoelectric materials, Int. Mater. Rev. 61 (6) (2016) 379–415.
[53] L. Huang, S. Xu, Z. Wang, K. Xue, J. Su, Y. Song, S. Chen, C. Zhu, B.Z. Tang, R. Ye, Self-Reporting and photothermally enhanced rapid bacterial killing on a laser-induced graphene mask, ACS Nano 14 (9) (2020) 12045–12053.
[54] M. Company, 3M™ Secure Click™ Reusable Half Mask HF-800 Serie, 2021. https://www.3m.co.uk/3M/en_GB/p/d/b5005081000/.
[55] M. Company, 3M™ Reusable Half Face Mask 6000 Series, 2021. https://www.3m.co.uk/3M/en_GB/p/d/sbgbpsd7001s/.
[56] Xupermask, Xupermask Features-Size and Weight, 2021. https://xupermask.com/specs/.